14th IEEE International Conference on Thermal, Mechanical & Multiphysics Simulation and Experiments in Micro/Nano-Electronics and Microsystems, EuroSimE 2013

The fracture studies of polycrystalline silicon based MEMS

15th April 2013

University of Liège
Shantanu S. Mulay, G. Becker, L. Noels

Université Catholique de Louvain
Renaud Vayrette, Jean-Pierre Raskin, Thomas Pardoen

Université Libre de Bruxelles
Montserrat Galceran, Stéphane Godet

Outline

- Introduction

- Numerical fracture framework for polycrystalline silicon
  - Discontinuous Galerkin (DG) method
  - Hybrid DG/Extrinsic cohesive law (ECL)
  - Orthotropic plane-stress Hooke's law for core of grains
  - Intra-granular fracture
  - Thickness effect
  - Preliminary results
  - Observations

- Future work
  - Characterize inter-granular strength
  - Compare with experiments
  - Apply to robust design

Introduction

- Purpose
  - Develop a numerical method to predict MEMS fracture
- Difficulties
  - Grains sizes are no longer negligible compared to the structure size
  - Silicon is anisotropic
  - Inter/intra granular fractures
  - Dimensions are not perfectly controlled
  - Two MEMS will have
    - Different grains orientations/sizes
    - Different dimensions/surface profiles
- The numerical method should thus be probabilistic
  - But impossible to perform many direct numerical simulations with grain size resolutions

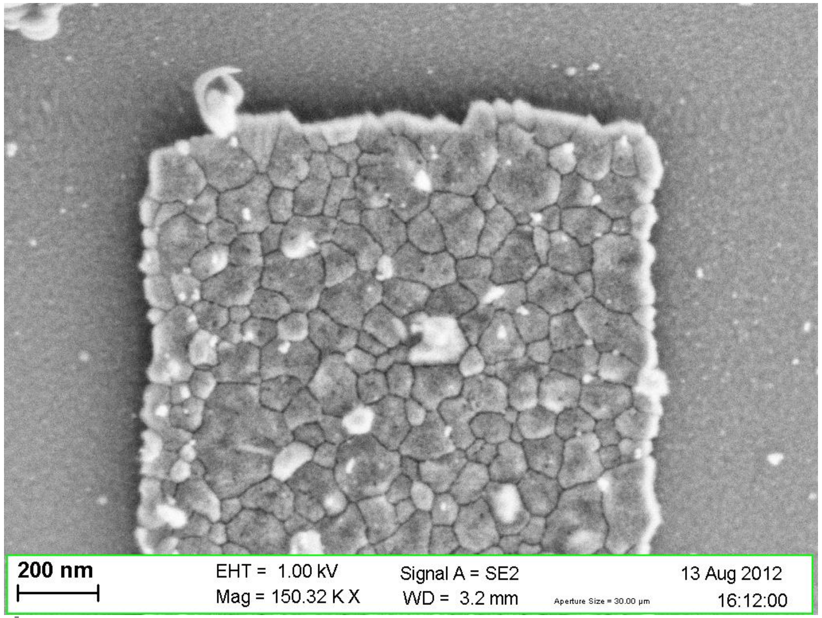

- Objective is to develop a robust design procedure of MEMS based on numerical stochastic 3-scale approaches

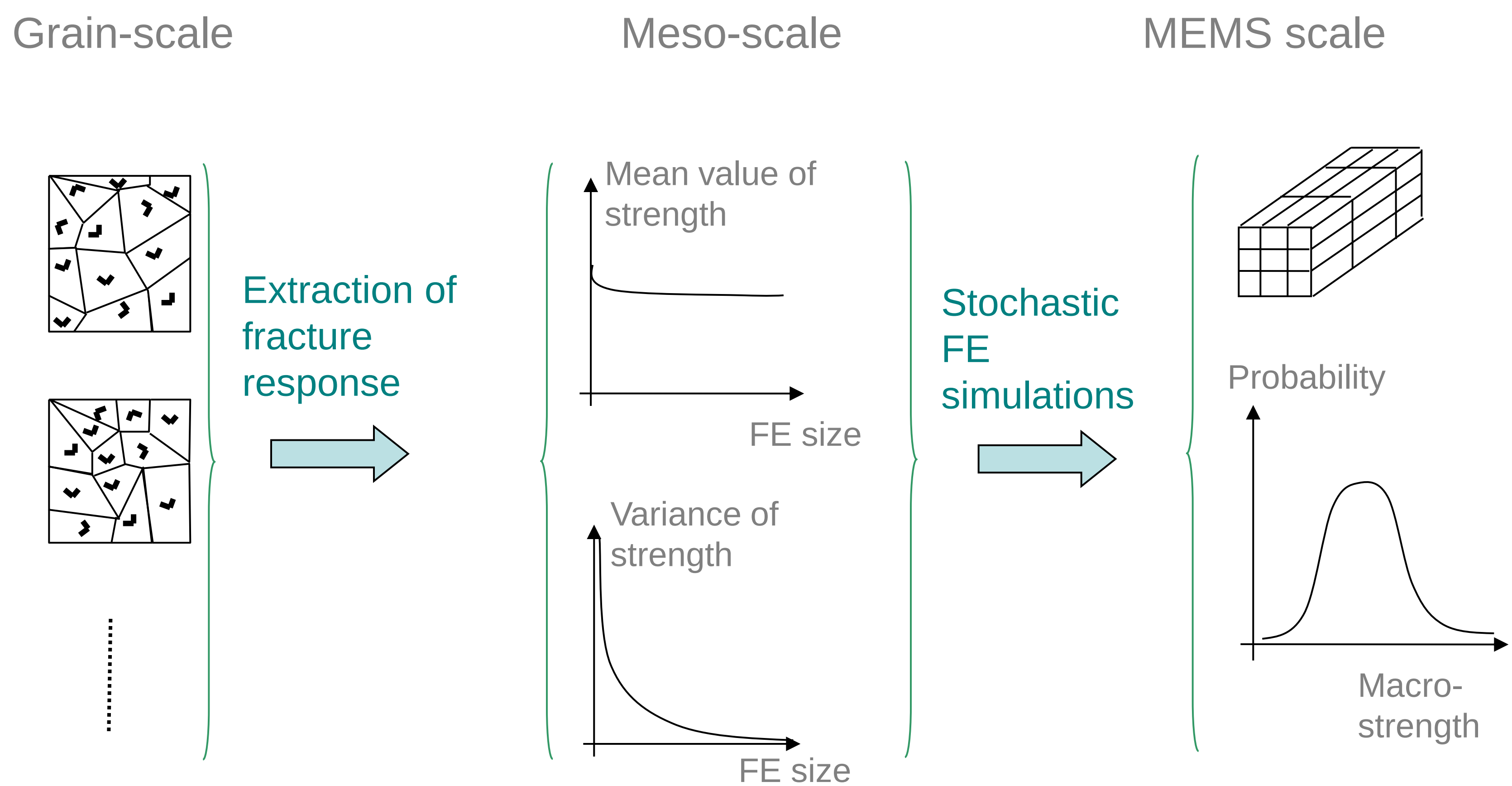

Introduction

- Methodology
  - Develop a numerical fracture framework for polycrystalline structures (ULg)
  - Validate tool with on-ship testing (UcL)

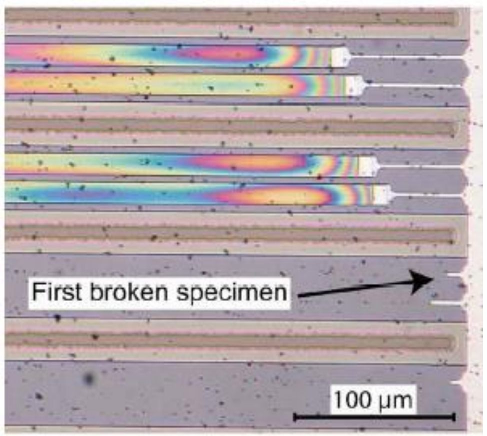

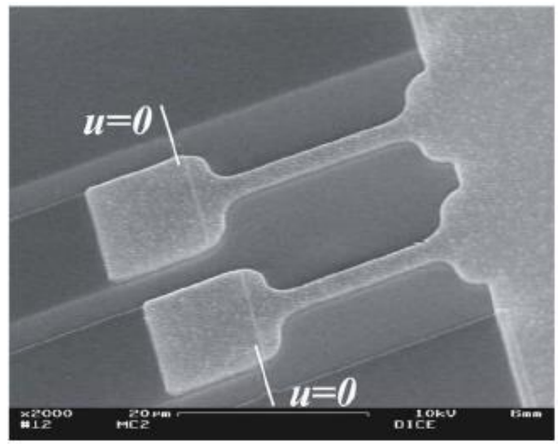

[Gravier et al., JMEMS 2009]

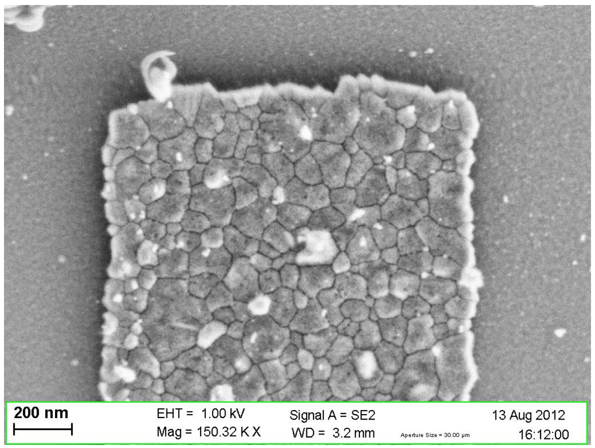

  - Exploit numerical fracture framework in the 3-scale stochastic method (future work)

Numerical fracture framework for polycrystalline silicon

- Fracture challenges
  - Fracture can be
    - Inter-granular
    - Intra-granular
  - Grains are anisotropic
  - Initially there is no crack

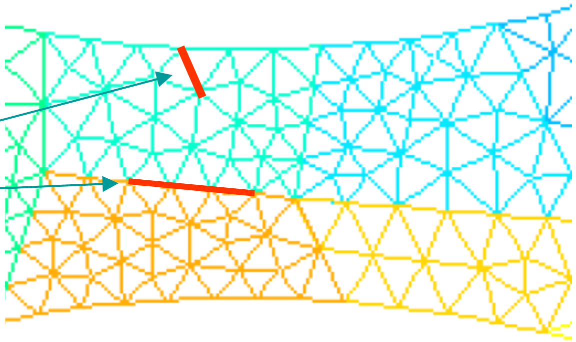

- Numerical approach
  - Cohesive elements inserted between two bulk elements
  - They integrate the cohesive Traction Separation Law
  - Characterized by
    - Strength σ_c &
    - Critical energy release rate G_C
  - Can be tailored for
    - Intra/inter granular failure
    - Different orientations

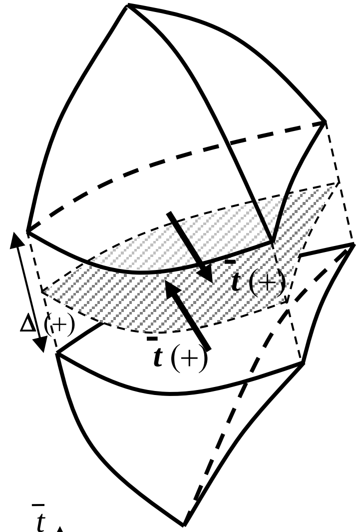

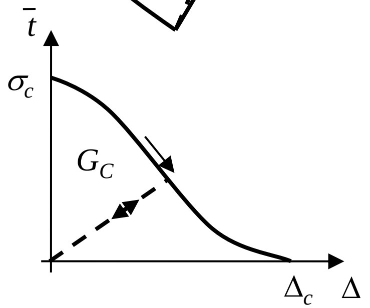

Numerical fracture framework for polycrystalline silicon

- Problems with cohesive elements
  - Intrinsic Cohesive Law (ICL)
    - Cohesive elements inserted from the beginning
    - Drawbacks:
      - Efficient if a priori knowledge of the crack path
      - Mesh dependency [Xu & Needelman, 1994]
      - Initial slope modifies the effective elastic modulus
      - This slope should tend to infinity [Klein et al. 2001]:
        - » Alteration of a wave propagation
        - » Critical time step is reduced
  - Extrinsic Cohesive Law (ECL)
    - Cohesive elements inserted on the fly when failure criterion is verified [Ortiz & Pandolfi 1999]
    - Drawback
      - Complex implementation in 3D (parallelization)

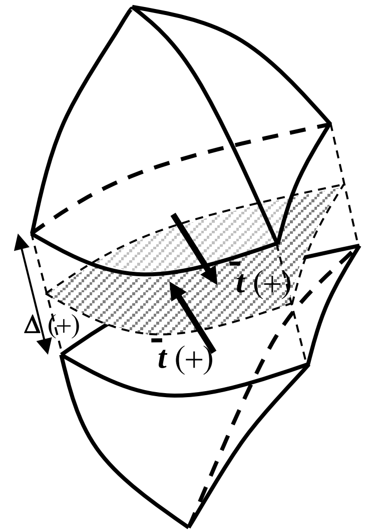

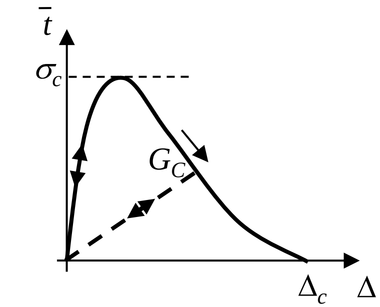

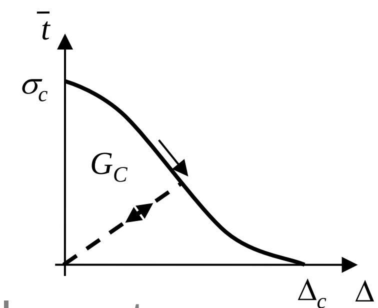

- Solution
  - Use discontinuous Galerkin method embedding interface elements

- Discontinuous Galerkin (DG) methods
  - Finite-element discretization
  - Same **discontinuous** polynomial approximations for the
    - **Test** functions φ_h and
    - **Trial** functions $\delta\varphi$

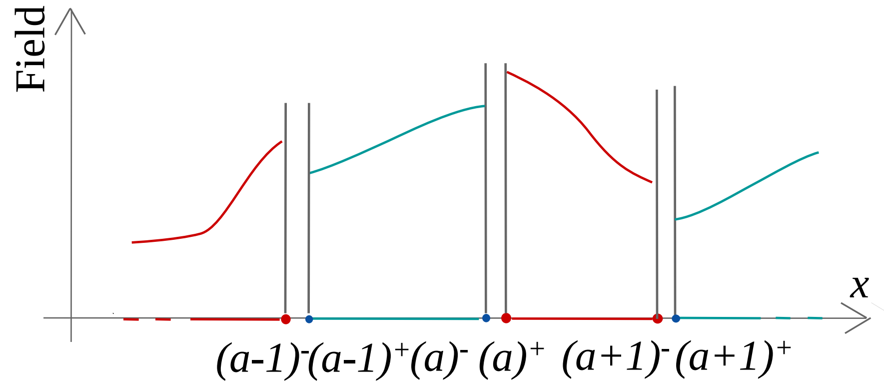

  - Definition of operators on the interface trace:
    - **Jump** operator: $[\![\bullet]\!] = \bullet^+ - \bullet^-$
    - **Mean** operator: $\langle\bullet\rangle = \dfrac{\bullet^+ + \bullet^-}{2}$
  - Continuity is weakly enforced, such that the method
    - Is consistent
    - Is stable
    - Has the optimal convergence rate

Numerical fracture framework for polycrystalline silicon

- Discontinuous Galerkin (DG) methods (2)
  - Formulation in terms of first Piola-Kirchhoff stress tensor $\mathbf{P}$

$$\boldsymbol{\nabla}_0 \cdot \mathbf{P}^T = 0 \text{ in } \Omega \quad \& \quad \begin{cases} \mathbf{P} \cdot \boldsymbol{N} = \bar{\boldsymbol{T}} \text{ on } \partial_N \Omega \\ \varphi_h = \bar{\varphi}_h \text{ on } \partial_D B \end{cases}$$

  - Weak formulation obtained by integration by parts **on each element** Ω^e

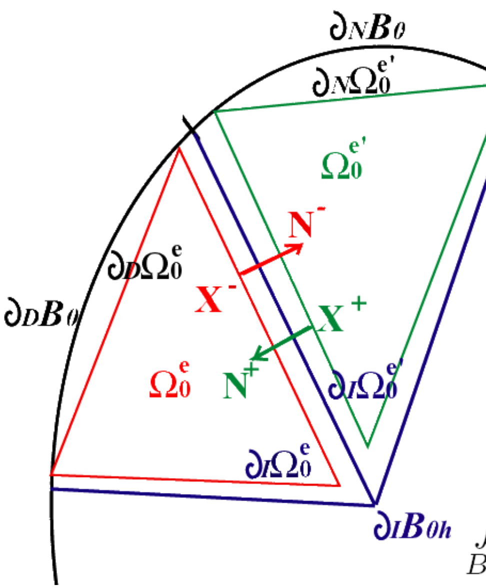

$$\sum_e \int_{\Omega_0^e} \boldsymbol{\nabla}_0 \cdot \mathbf{P}^T (\varphi_h) \cdot \delta\varphi \, dB = 0$$

$$\sum_e \int_{\Omega_0^e} -\mathbf{P}(\varphi_h) : \boldsymbol{\nabla}_0 \delta\varphi \, dB + \sum_e \int_{\partial\Omega_0^e} \delta\varphi \cdot \mathbf{P}(\varphi_h) \cdot \boldsymbol{N} \, d\partial B = 0$$

$$\int_{B_0} \mathbf{P}(\varphi_h) : \boldsymbol{\nabla}_0 \delta\varphi \, dB + \int_{\partial_I B_0} [\![\delta\varphi \cdot \mathbf{P}(\varphi_h)]\!] \cdot \boldsymbol{N}^- \, d\partial B = \int_{\partial_N B_0} \bar{\boldsymbol{T}} \cdot \delta\varphi \, d\partial B$$

New interface terms

- Discontinuous Galerkin (DG) methods (3)
  - Interface terms rewritten as the sum of 3 terms
  - Introduction of the numerical flux $\boldsymbol{h}$

$$\int_{\partial_I B_0} [\![\delta\boldsymbol{\varphi} \cdot \mathbf{P}(\boldsymbol{\varphi}_h)]\!] \cdot \boldsymbol{N}^- \, d\partial B \rightarrow \int_{\partial_I B_0} [\![\delta\boldsymbol{\varphi}]\!] \cdot \boldsymbol{h}\left(\mathbf{P}^+, \mathbf{P}^-, \boldsymbol{N}^-\right) \, d\partial B$$

    - Has to be consistent: $\begin{cases} \boldsymbol{h}\left(\mathbf{P}^+, \mathbf{P}^-, \boldsymbol{N}^-\right) = -\boldsymbol{h}\left(\mathbf{P}^-, \mathbf{P}^+, \boldsymbol{N}^+\right) \\ \boldsymbol{h}\left(\mathbf{P}_{\text{exact}}, \mathbf{P}_{\text{exact}}, \boldsymbol{N}^-\right) = \mathbf{P}_{\text{exact}} \cdot \boldsymbol{N}^- \end{cases}$
    - One possible choice: $\boldsymbol{h}\left(\mathbf{P}^+, \mathbf{P}^-, \boldsymbol{N}^-\right) = \langle \mathbf{P} \rangle \cdot \boldsymbol{N}^-$
  - Weak enforcement of the compatibility

$$\int_{\partial_I B_0} [\![\boldsymbol{\varphi}_h]\!] \cdot \left\langle \frac{\partial \mathbf{P}}{\partial \mathbf{F}} : \boldsymbol{\nabla}_0 \delta\boldsymbol{\varphi} \right\rangle \cdot \boldsymbol{N}^- \, d\partial B$$

  - Stabilization controlled by parameter β, for all mesh sizes h^s

$$\int_{\partial_I B_0} [\![\boldsymbol{\varphi}_h]\!] \otimes \boldsymbol{N}^- : \left\langle \frac{\beta}{h^s} \frac{\partial \mathbf{P}}{\partial \mathbf{F}} \right\rangle : [\![\delta\boldsymbol{\varphi}]\!] \otimes \boldsymbol{N}^- \, d\partial B$$

  - Can also be explicitly derived from a variational form [Noels & Radovitzky, IJNME 2006 & JAM 2006]

Numerical fracture framework for polycrystalline silicon

- Hybrid DG/ECL
  - Interface terms exist at the beginning
    - DG method ensures consitency/stability
      [Seagraves, Jerusalem, Radovitzky, Noels, CMAME 2012]

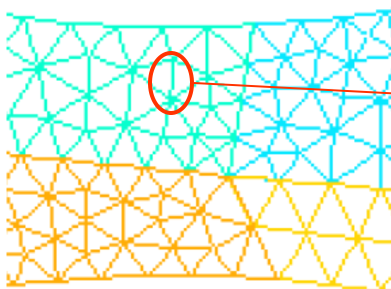

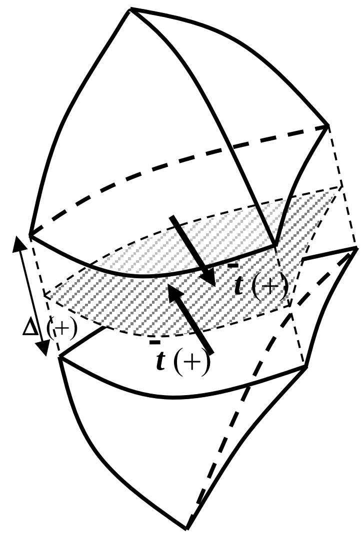

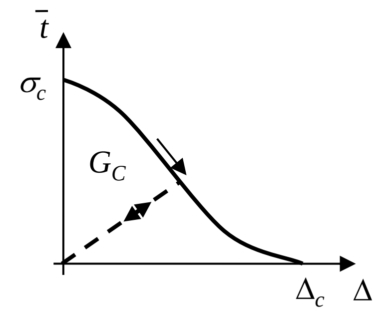

  - Onset of fracture
    - When interface traction reaches σ_c
    - The cohesive law substitutes for the DG terms
  - Advantages
    - Consistent
    - Easy to implement
    - Highly parallelizable
- In this work 2D plane-stress structures are studied

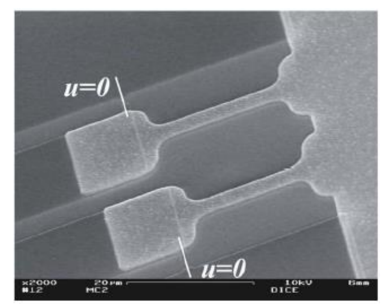

Numerical fracture framework for polycrystalline silicon

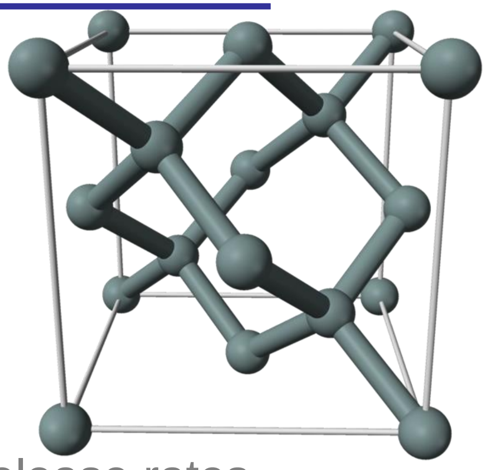

- Silicon crystal
  - Diamond-cubic crystal
  - Has symmetry-equivalent surfaces
  - Orthotropic material (at least two orthogonal planes of symmetry)
  - Different fracture strengths and critical strain energy release rates along crystal lattice planes
    - 6 {1 0 0}-directions, 12 {1 1 0}-directions, 8 {1 1 1}-directions

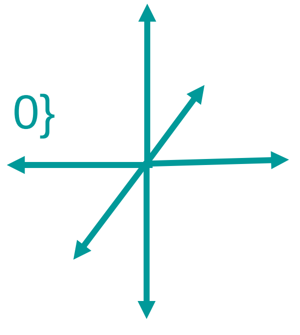

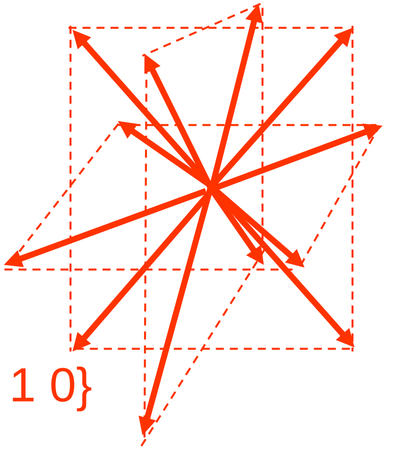

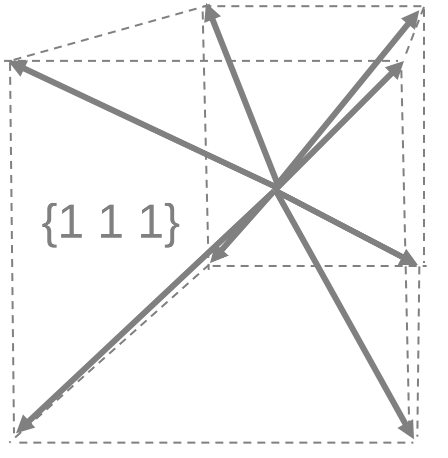

$$\sigma_{100} = 1.53\ \mathrm{GPa}, \sigma_{110} = 1.21\ \mathrm{GPa}, \sigma_{111} = 0.868\ \mathrm{GPa}$$

Numerical fracture framework for polycrystalline silicon

- Bulk law
  - In the referential (x, y, z) of the crystal
    - 9 constants (actually 3 ≠)

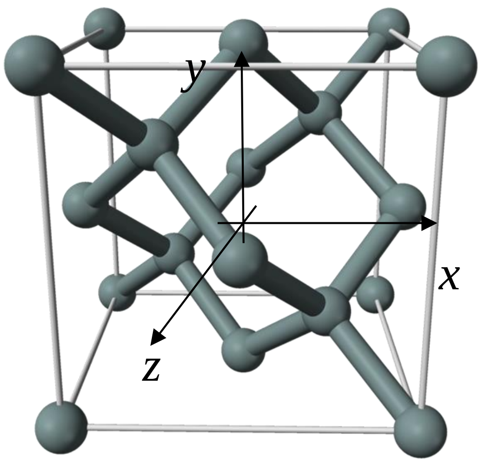

$$\left\{\begin{array}{c}\epsilon_{xx}\\ \epsilon_{yy}\\ \epsilon_{zz}\\ \epsilon_{xy}\\ \epsilon_{yz}\\ \epsilon_{zx}\end{array}\right\} = \left[\begin{array}{cccccc} \frac{1}{E_x} & \frac{-\nu_{yx}}{E_y} & \frac{-\nu_{zx}}{E_z} & 0 & 0 & 0\\ \frac{-\nu_{xy}}{E_x} & \frac{1}{E_y} & \frac{-\nu_{zy}}{E_z} & 0 & 0 & 0\\ \frac{-\nu_{xz}}{E_x} & \frac{-\nu_{yz}}{E_y} & \frac{1}{E_z} & 0 & 0 & 0\\ 0 & 0 & 0 & \frac{1}{2G_{xy}} & 0 & 0\\ 0 & 0 & 0 & 0 & \frac{1}{2G_{yz}} & 0\\ 0 & 0 & 0 & 0 & 0 & \frac{1}{2G_{zx}} \end{array}\right] \left\{\begin{array}{c}\sigma_{xx}\\ \sigma_{yy}\\ \sigma_{zz}\\ \sigma_{xy}\\ \sigma_{yz}\\ \sigma_{zx}\end{array}\right\}$$

  - Is rotated in the referential axes (X, Y, Z)
    - Different angles for different grains
    - Plane stress state $\sigma_{ZZ} = 0$

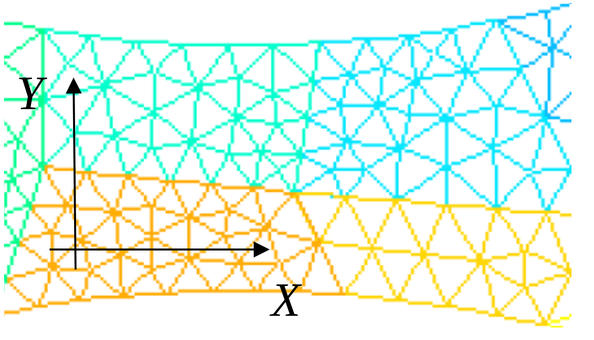

Numerical fracture framework for polycrystalline silicon

- Intra-granular fracture
  - Different fracture strengths along crystal lattice planes
    - 6 {1 0 0}-directions $\hat{n}_1$, 12 {1 1 0}-directions $\hat{n}_2$, 8 {1 1 1}-directions $\hat{n}_3$
  - Mesh-interfaces are not along a fracture direction

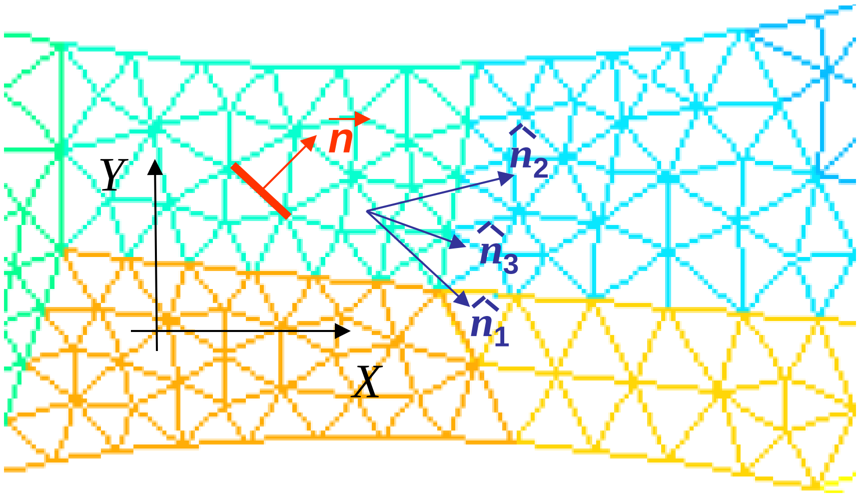

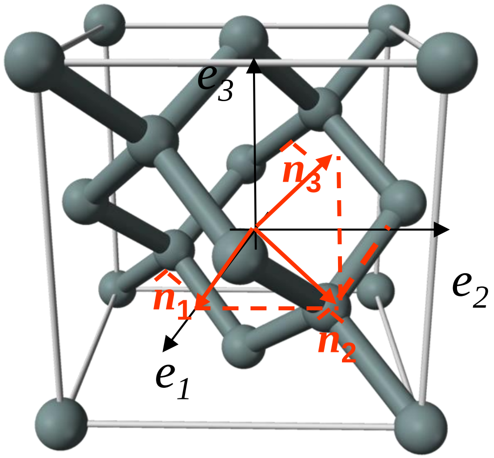

- Assumption: FE mesh > silicon crystal cell size (5.43 Å)
  - Compute effective fracture strength on any required plane
- But: $\hat{n}_1$, $\hat{n}_2$ & $\hat{n}_3$ do not form an orthonormal basis
  - Consider the dual basis $\hat{n}^1$, $\hat{n}^2$ & $\hat{n}^3$

Numerical fracture framework for polycrystalline silicon

- Intra-granular fracture (2)
  - Surface normals of (1 0 0), (1 1 0), (1 1 1) known
    - $\hat{n}_1$, $\hat{n}_2$ & $\hat{n}_3$ do not form an orthonormal basis
    - Consider the dual basis $\hat{n}^1$, $\hat{n}^2$ & $\hat{n}^3$

$$\left.\begin{aligned} \hat{n}_1 &= \hat{e}_1 \\ \hat{n}_2 &= (1/\sqrt{2})(\hat{e}_1+\hat{e}_2) \\ \hat{n}_3 &= (1/\sqrt{3})(\hat{e}_1+\hat{e}_2+\hat{e}_3) \end{aligned}\right\} \Rightarrow \quad \begin{aligned} \hat{n}^1 &= \hat{e}_1 - \hat{e}_2 \\ \hat{n}^2 &= \sqrt{2}(\hat{e}_2 - \hat{e}_3) \\ \hat{n}^3 &= \sqrt{3}\,\hat{e}_3 \end{aligned}$$

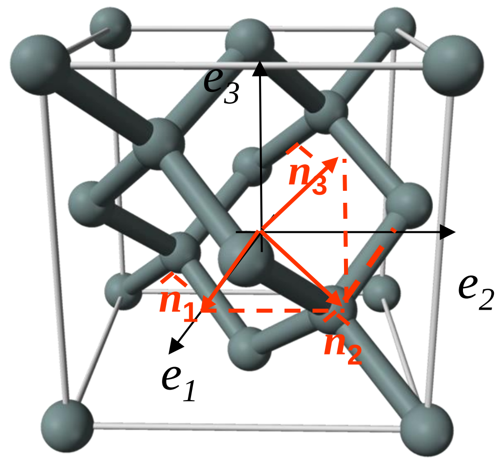

- Extract component of surface normal in the dual basis

$$\begin{cases} n^{100} = \vec{n}\cdot\hat{n}^1 \\ n^{110} = \vec{n}\cdot\hat{n}^2 \\ n^{111} = \vec{n}\cdot\hat{n}^3 \end{cases}$$

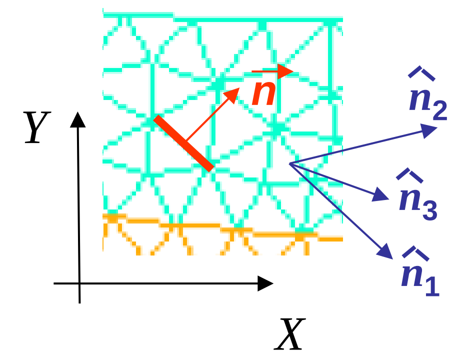

- Interpolate strength from strength along {1 0 0}, {1 1 0} and {1 1 1}

$$\vec{\sigma}_{eff} = \left[\sigma_{100}\, n^{100} + \frac{\sigma_{110}\, n^{110}}{\sqrt{2}} + \frac{\sigma_{111}\, n^{111}}{\sqrt{3}}\right]\hat{e}_1 + \left[\frac{\sigma_{110}\, n^{110}}{\sqrt{2}} + \frac{\sigma_{111}\, n^{111}}{\sqrt{3}}\right]\hat{e}_2 + \left[\frac{\sigma_{111}\, n^{111}}{\sqrt{3}}\right]\hat{e}_3$$

Numerical fracture framework for polycrystalline silicon

- Intra-granular fracture (3)
  - At the end of the day
    - $\sigma_{100} = 1.53\ \mathrm{GPa}, \sigma_{110} = 1.21\ \mathrm{GPa}, \sigma_{111} = 0.868\ \mathrm{GPa}$
    - $\|\vec{\sigma}_{eff}\| = \sqrt{\left(\sigma_{100}\, n^{100} + \frac{\sigma_{110}\, n^{110}}{\sqrt{2}} + \frac{\sigma_{111}\, n^{111}}{\sqrt{3}}\right)^2 + \left(\frac{\sigma_{110}\, n^{110}}{\sqrt{2}} + \frac{\sigma_{111}\, n^{111}}{\sqrt{3}}\right)^2 + \left(\frac{\sigma_{111}\, n^{111}}{\sqrt{3}}\right)^2}$
    - Applicable when surface normal is in-between solid angle formed by $\hat{\boldsymbol{n}}_1$, $\hat{\boldsymbol{n}}_2$ & $\hat{\boldsymbol{n}}_3$
    - 48 solid angles are identified in $\theta \in [0, 360]$ and $\phi \in [0, 180]$

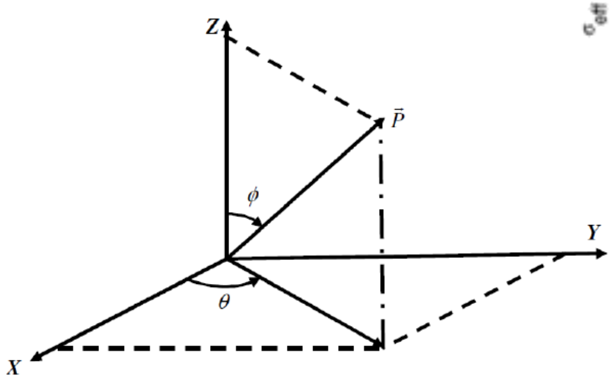

Spherical coordinate system

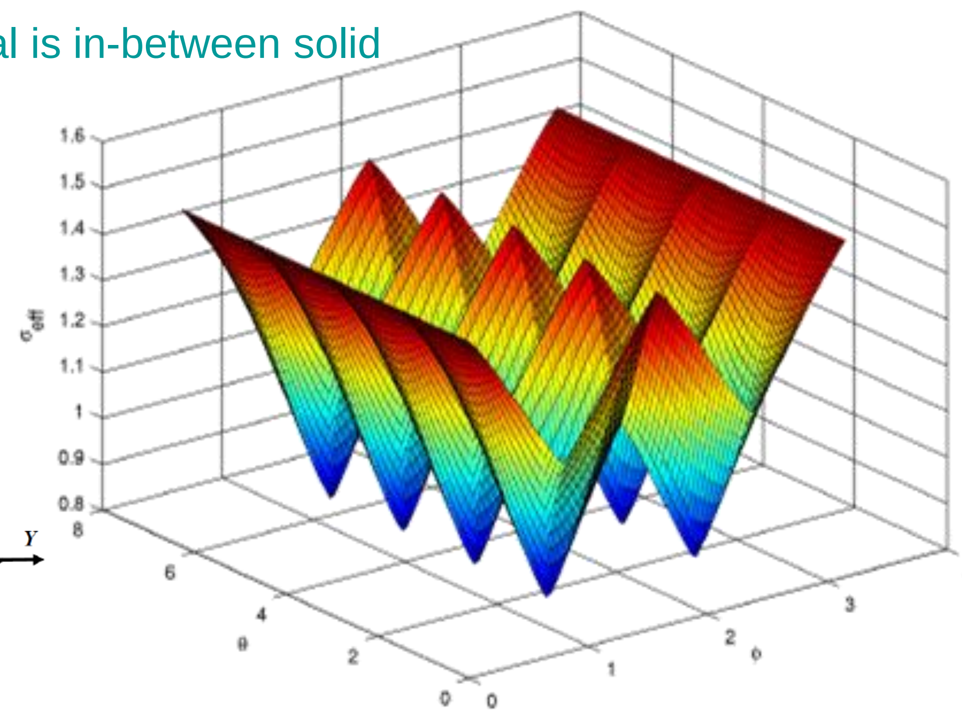

Numerical fracture framework for polycrystalline silicon

- Thickness effect
  - 2D-plane-stress model
  - Reality is 3D
    - Anisotropy
    - Weakest plane is not always the section
  - Find weakest plane passing through the interface edge
    - Iterate on θ
    - Compute new edge referential

$$\left\{ \begin{array}{c} \hat{n}' \\ \hat{t}_0' \\ \hat{t}' \end{array} \right\} = \left[\begin{array}{ccc} \cos(\theta) & \sin(\theta) & 0 \\ -\sin(\theta) & \cos(\theta) & 0 \\ 0 & 0 & 1 \end{array} \right] \left\{ \begin{array}{c} \hat{n} \\ \hat{t}_0 \\ \hat{t} \end{array} \right\}$$

    - Compute normal and tangential stress in new referential

$$\left. \begin{array}{r} \mathrm{S_{nor}} = (\sigma\, \hat{n}) \cdot \hat{n}' , \tau = (\sigma\, \hat{n}) \cdot \hat{t}' \\ \tau_0 = (\sigma\, \hat{n}) \cdot \hat{t}_0' , \tau_{\mathrm{resultant}} = \sqrt{(\tau)^2 + (\tau_0)^2} \end{array} \right\}$$

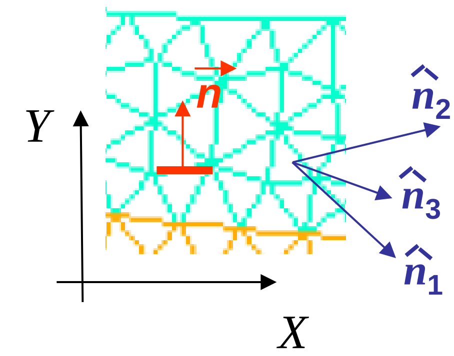

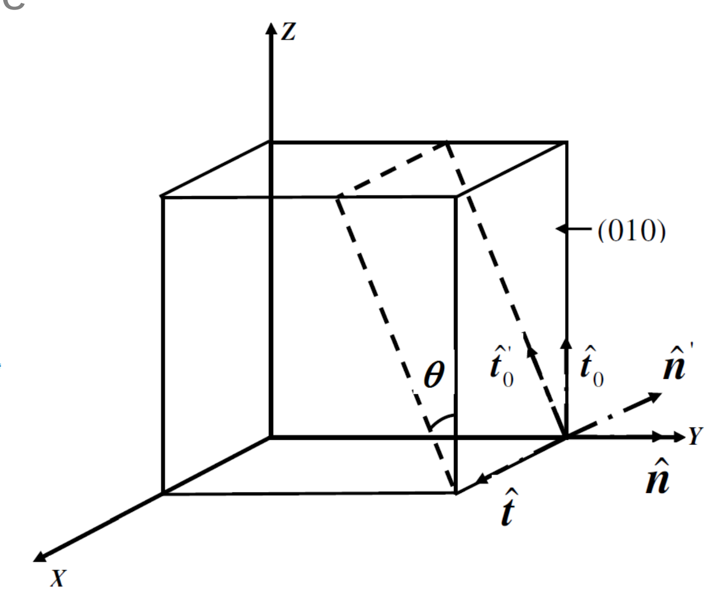

Rotation of interface element along the thickness of MEMS

Numerical fracture framework for polycrystalline silicon

- Thickness effect (2)
  - Find weakest plane passing through the interface edge (2)
    - Compute effective stress in the new referential

$$\mathrm{S}_{eff} = \begin{cases} \sqrt{\left(\mathrm{S}_{\mathrm{nor}}\right)^2 + \left(\beta\right)^{-2}\left(\tau_{\mathrm{resultant}}\right)^2}, & \text{if } \mathrm{S}_{\mathrm{nor}} \geq 0 \\ \dfrac{1}{\beta}\left\langle\left\langle\left|\tau_{\mathrm{resultant}}\right| - \mu_c\left|\mathrm{S}_{\mathrm{nor}}\right|\right\rangle\right\rangle, & \text{if } \mathrm{S}_{\mathrm{nor}} < 0 \end{cases}$$

[Camacho & Ortiz, IJSS 1996]

    - Compare this value to effective fracture strength along $\hat{n}$,
    - Extrapolated as previously

Preliminary results

- MEMS modelled by 9 crystal lattices with 534 elements
- Solved without and with thickness effect

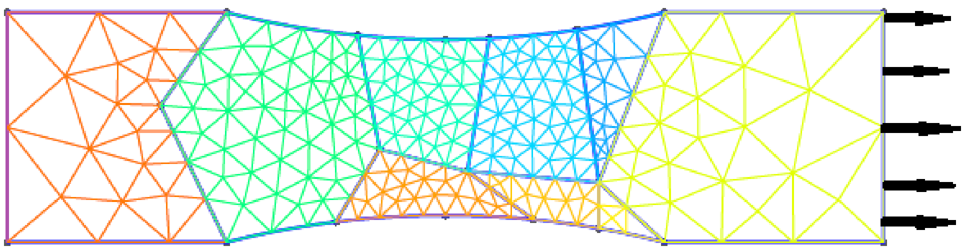

MEMS geometry

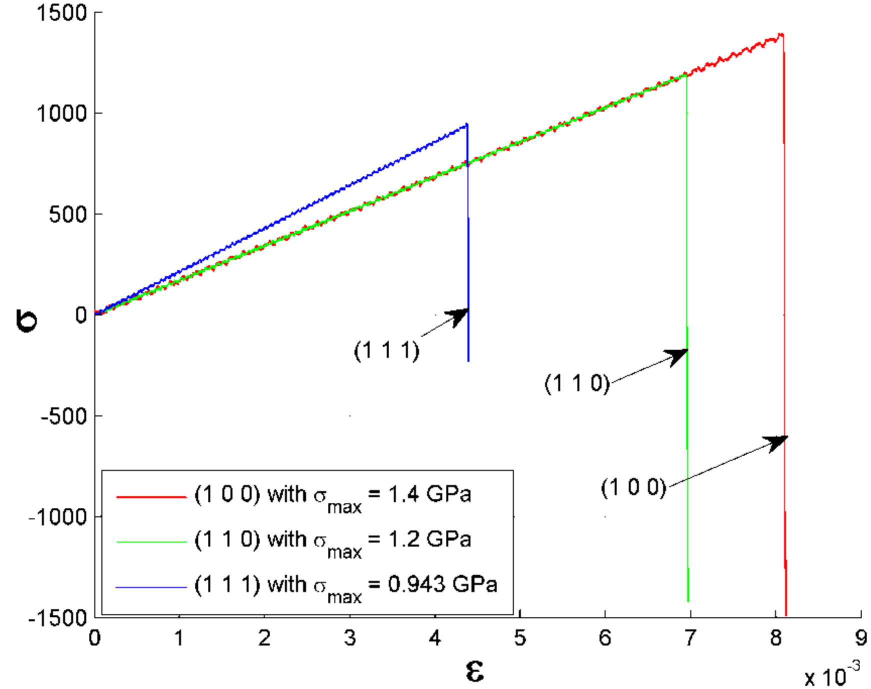

Stress vs. strain plots along right boundary without thickness effect

$$\sigma_{100} = 1.53\ \mathrm{GPa}, \sigma_{110} = 1.21\ \mathrm{GPa}, \sigma_{111} = 0.868\ \mathrm{GPa}$$

$$\mathrm{Gc}_{100} = 2.54, \mathrm{Gc}_{110} = 2.10, \mathrm{Gc}_{111} = 1.28\ \mathrm{J/m^2}$$

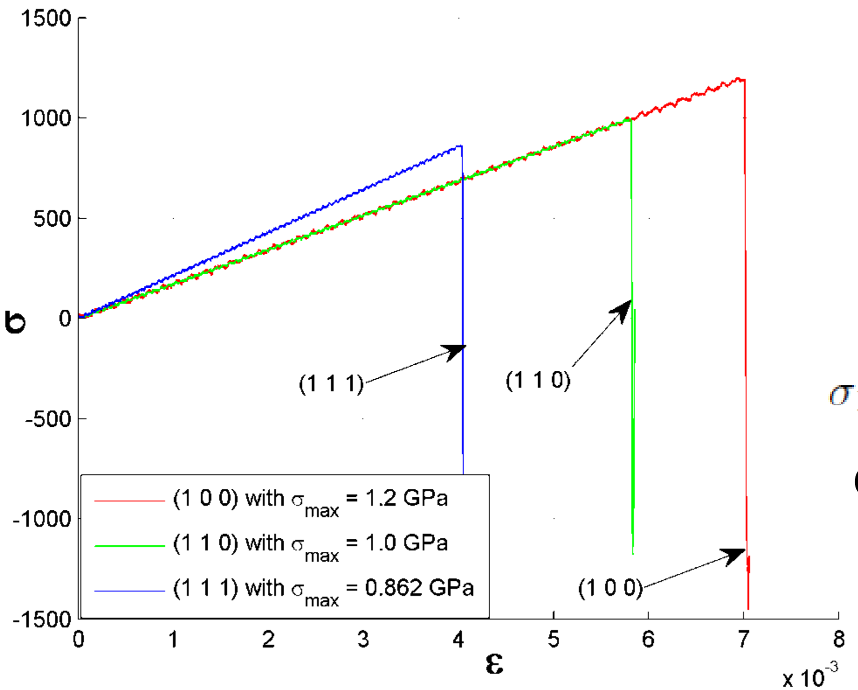

Stress vs. strain plots along right boundary with thickness effect

Preliminary results (2)

Crack tip stress at the beginning of first fracture

Orientation	Normal stress (without thickness)(GPa)	Normal stress (with thickness)
(1 0 0)	1.43	1.24
(1 1 0)	1.23	1.03
(1 1 1)	0.985	0.909

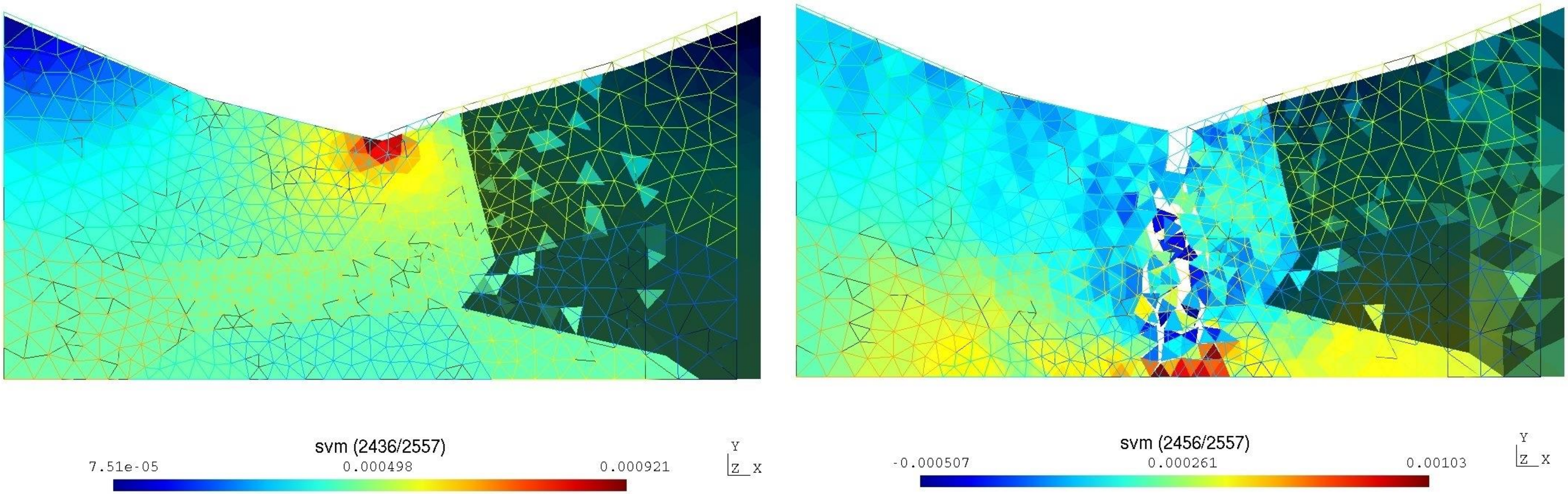

a **b**

(a) commencement and (b) end of the through-the-thickness fracture of MEMS with a v-notch when all the crystals are oriented along (1 1 0) direction

Experimental observations

- On-chip tensile microstructure fabricated to test MEMS for fracture
  - Extraction of Young's modulus and fracture strain by SEM and TEM
  - Automated crystallographic orientation mapping on transmission electron microscope (ACOM-TEM) technique to determine local orientations of grains

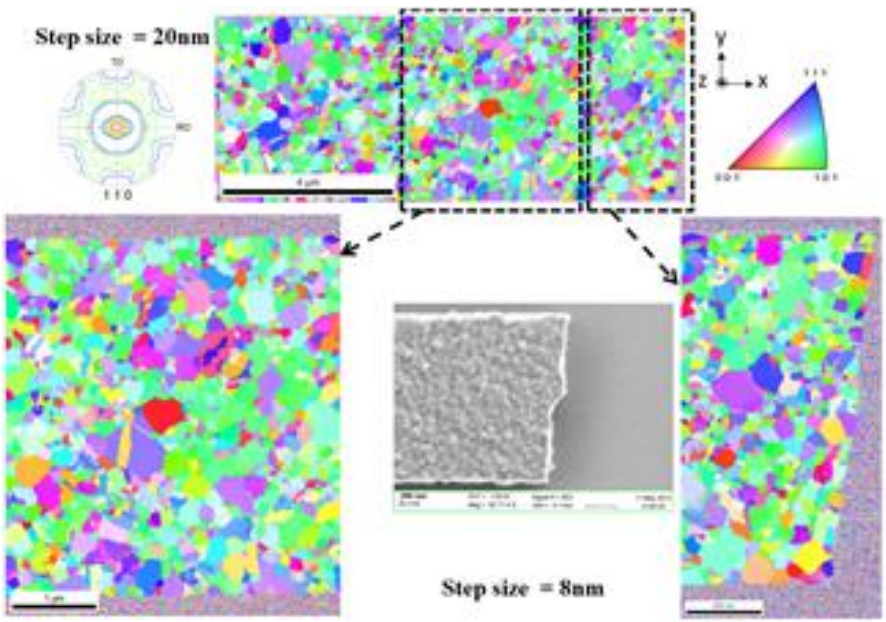

a

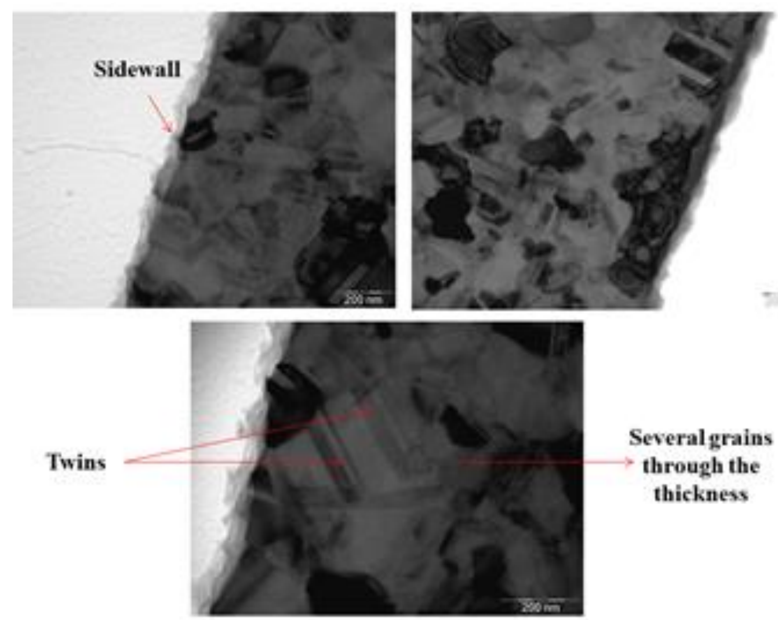

b

(a) Top view of the out-of-plane orientation map of 240 nm-thick polysilicon sample and (b) bright field TEM image of polysilicon sample

Experimental observations continued …

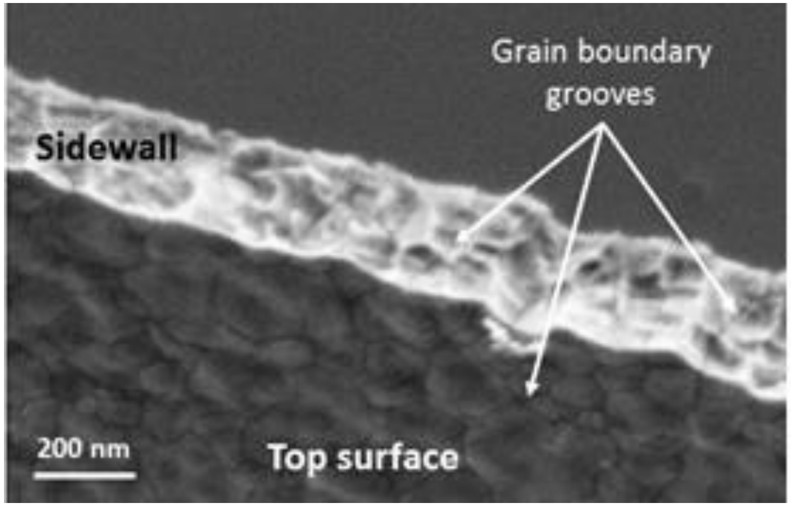

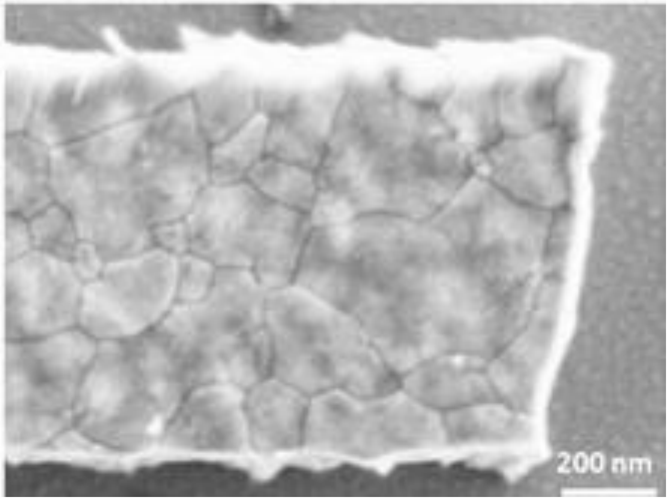

a **b**

(a) SEM image of the side wall of 240 nm-thick polysilicon sample and (b) SEM image of the top view of fracture zone of polysilicon sample

- SEM observation shows the presence of one or two grains along the thickness of sample
- Average local preferential orientation (1 1 0) in the out-of-plane direction and in-plane orientations are random
- Fracture initiated due to the flaws on sidewalls created during sample preparation

Observations

- Maximum stresses along the loading edge and crack tip are close to effective fracture strength
  - Validate the correctness of the computation of effective fracture strength
- Maximum fracture stress at crack tip is slightly lower with thickness effect as compared with without thickness effect
  - Maximum stress at fracture is either S_{nor} or τ
  - First fracture is detected when $S_{eff} \geq \sigma_{(111)}$
  - Irrespective of the orientation of crystal lattices, there will be at least one interface plane orientated in the direction (1 1 1)
  - Verifies experimental observation that, independent of the orientation of crystal lattices, crack propagates in the direction (1 1 1)
  - $\sigma_{\max}(100) \geq \sigma_{\max}(110) \geq \sigma_{\max}(111)$, as (111) is weakest plane

Observations continued …

- Experimentally observed fracture strain 0.96% (+/- 0.07%) and fracture stress 1.41 (+/- 0.1) GPa
  - fracture stress in between the fracture strengths along (1 0 0) and (1 1 0) cleavage planes, as these planes influence in-plane fracture behaviour
- Numerically observed fracture strain 0.7% (+/- 0.1%) and fracture stress 1.1 (+/- 0.1) GPa
  - Fracture stress is slightly lower than experimentally observed value
  - Effective fracture strength is computed by weighted average values of fracture strengths along the (1 0 0), (1 1 0), and (1 1 1) orientations
  - Experimental sample has random in-plane orientations with higher influence of (1 0 0) and (1 1 0) orientations
- Transgranular crack path

Future work

- Inter-granular strength
  - Characterize strength
  - In terms of mis-orientations
- Compare with experiments
  - Grains orientations by automated crystal oriented mapping (ACOM)
  - Analysis of the competition between inter-granular versus trans-granular crack path with respect to grain orientation

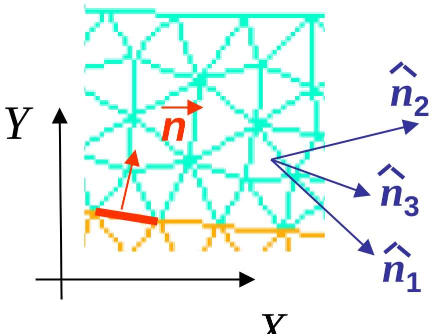

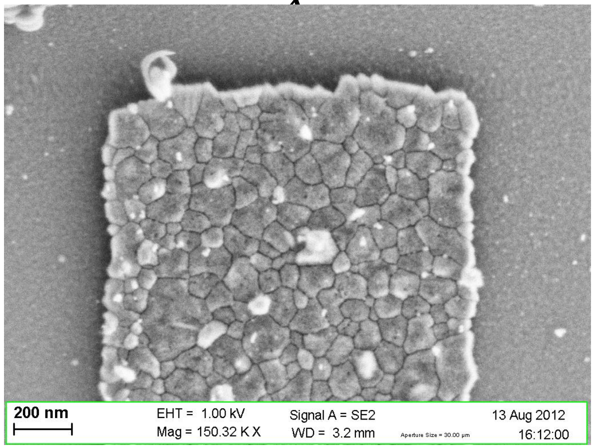

Future work

- Robust-design
  - Statistical fracture strength at meso-scale from micro-scale simulations involving different grain sizes and grain orientations
  - Stochastic numerical method considering statistical distribution of fracture strength

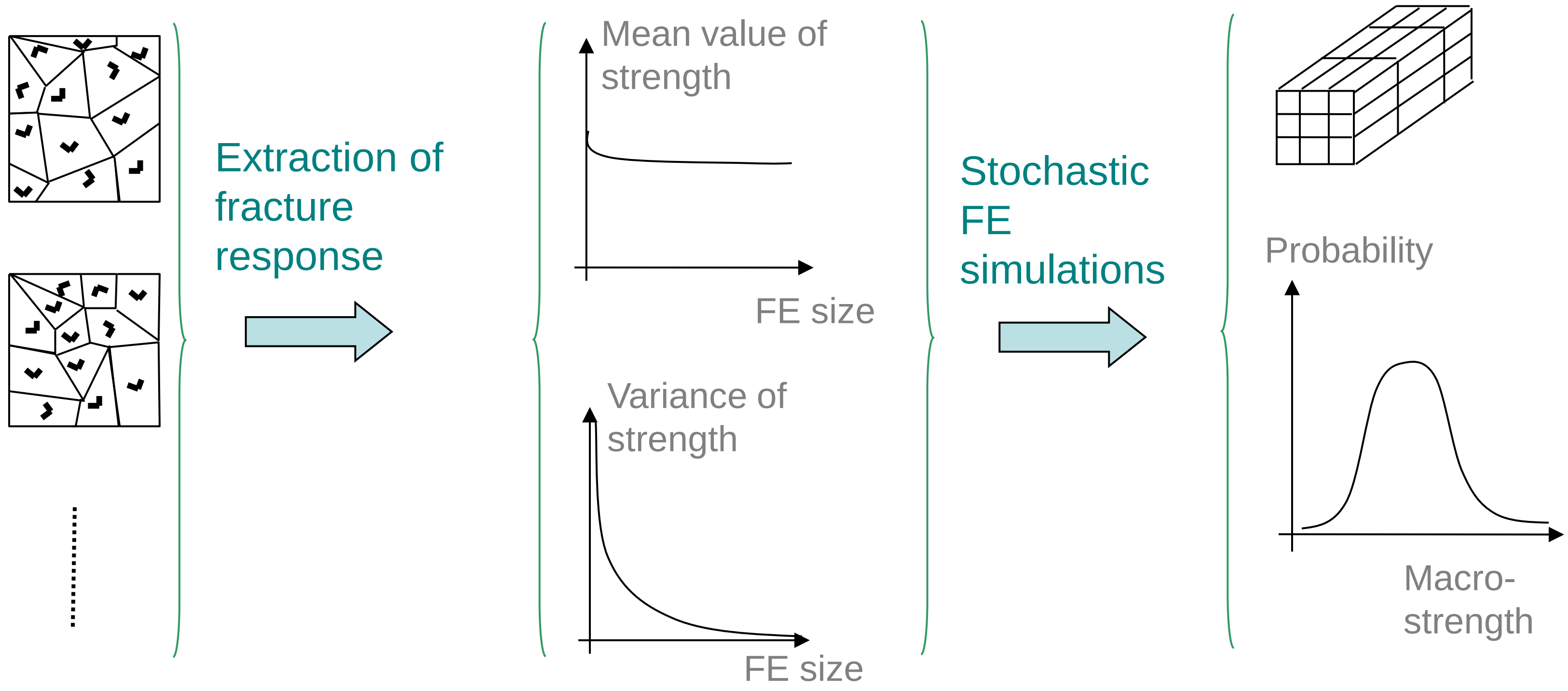

Thank you